

**Wave cloud**

Z. Cui et al.

This discussion paper is/has been under review for the journal Atmospheric Chemistry and Physics (ACP). Please refer to the corresponding final paper in ACP if available.

# Aircraft measurements of wave cloud

Z. Cui<sup>1</sup>, A. M. Blyth<sup>1,2</sup>, K. N. Bower<sup>3</sup>, J. Crosier<sup>2,3</sup>, and T. Choularton<sup>3</sup>

<sup>1</sup>Institute for Climate and Atmospheric Science, School of Earth and Environment, University of Leeds, UK

<sup>2</sup>National Centre for Atmospheric Science, UK

<sup>3</sup>Centre for Atmospheric Science, SEAES, University of Manchester, UK

Received: 6 March 2012 – Accepted: 8 May 2012 – Published: 29 May 2012

Correspondence to: Z. Cui (z.cui@leeds.ac.uk)

Published by Copernicus Publications on behalf of the European Geosciences Union.

Title Page

Abstract

Introduction

Conclusions

References

Tables

Figures

◀

▶

◀

▶

Back

Close

Full Screen / Esc

Printer-friendly Version

Interactive Discussion



## Abstract

In this paper, aircraft measurements are presented of liquid phase (ice-free) wave clouds made at temperatures greater than  $-5^{\circ}\text{C}$  that formed over Scotland, UK. The horizontal variations of the vertical velocity across wave clouds display a distinct pattern. The maximum updraughts occur at the upshear flanks of the clouds and the strong downdraughts at the downshear flanks. The cloud droplet concentrations were a couple of hundreds per cubic centimetres, and the drops generally had a mean diameter between 15–45  $\mu\text{m}$ . A small proportion of the drops were drizzle. A new definition of a mountain-wave cloud is given, based on the measurements presented here and previous studies. The results in this paper provide a case for future numerical simulation of wave cloud and the interaction between wave and clouds.

## 1 Introduction

Wave clouds are produced when air passes over obstacles such as mountains or islands in specific environmental conditions. The classical problem of small amplitude, two-dimensional mountain waves can be analyzed with the Scorer parameter (Scorer, 1949)

$$I^2 = \left(\frac{N}{U}\right)^2 - \frac{1}{U} \left(\frac{d^2U}{dz^2}\right)^2, \quad (1)$$

where  $N$  is the Brunt Väisälä frequency,  $U$  is the mean wind speed of the flow normal to the mountain, and  $z$  is the height above ground. The Scorer parameter is used to distinguish flow regimes. In the regime of large Scorer parameter (i.e., the Scorer parameter  $>$  wavelength), buoyancy force plays a more important role than horizontal advection. The time an air parcel takes to pass over the orography is greater than it takes for vertical oscillation due to atmospheric stratification. In this case, mountain

ACPD

12, 13337–13362, 2012

## Wave cloud

Z. Cui et al.

Title Page

Abstract

Introduction

Conclusions

References

Tables

Figures

◀

▶

◀

▶

Back

Close

Full Screen / Esc

Printer-friendly Version

Interactive Discussion



**Wave cloud**

Z. Cui et al.

[Title Page](#)[Abstract](#)[Introduction](#)[Conclusions](#)[References](#)[Tables](#)[Figures](#)[Back](#)[Close](#)[Full Screen / Esc](#)[Printer-friendly Version](#)[Interactive Discussion](#)

waves can be supported. Although linear theories have provided a concise and clear picture of mountain waves (e.g., Wood, 2000), they cannot describe large-amplitude waves which are related to wave clouds. In addition, moist processes are not considered in simple theoretical studies. Cotton et al. (2010) and Lin (2007) describe the problems of classical mountain waves, such as nonlinear waves, the effect of moist processes, and three-dimensionality of terrains. A number of unique wave cloud types are observed over and near mountains: cap clouds, banner clouds, lenticular clouds and lee wave clouds (Ludlam, 1980). Wave clouds attract research in cloud microphysics for two reasons. First, the thermodynamic and kinematic conditions of wave clouds are relatively steady during their life times. Second, the ranges of temperature, humidity, and vertical velocity of wave clouds are similar to laboratory-like settings, especially for ice formation and development (e.g., Baker and Lawson, 2006). For those reasons, previous wave cloud studies have focused on the ice nuclei and ice particles, particularly lenticular clouds because of the stationary feature with respect to the mountain (e.g., Cooper and Saunders, 1980; Cooper and Vali, 1981; Politovich and Vali, 1983; Twohy et al., 1997; Baumgardner and Gandrud, 1998; Jensen et al., 1998; Field et al., 2001; Baker and Lawson, 2006).

Moist processes can influence flow induced by mountain waves because condensational heating and evaporative cooling can alter atmospheric stratification (Cotton et al., 2010). The inclusion of moist processes generally weakens the amplitude of mountain waves (Durran and Klemp, 1982). Moreover, the interaction between mountain waves and clouds can influence the organization of clouds (Clark et al., 1986; Kuettner et al., 1987).

Gravity waves play an important role in cloud organisation (e.g., Clark, 1986; Clark and Hauf, 1986; Kuettner et al., 1987). Clark et al. (1986) and Clark and Hauf (1986) found that boundary layer eddies and cumulus clouds can excite gravity waves that propagate horizontally and vertically. The boundary layer eddies perturb the capping inversion and induce gravity waves. Cumulus clouds act as obstacles in the flow with wind shear, develop positive pressure perturbations on the upshear flanks and negative

pressure perturbations on the downshear flank, and excite gravity waves. The excited gravity waves can feedback on the boundary layer eddies, causing a change in the spacing of cloud lines.

A mountain-wave cloud is defined as “a cloud that forms in the rising branches of mountain waves and occupies the crests of the waves” (Glickman, 2000). However, in a study of the effect of moisture on mountain waves, Durran and Klemp (1982) showed that cloudy regions occurred in the wave crests (i.e., between strongest updraught and strongest downdraught) with ambient relative humidity  $RH = 90\%$ . The vertical velocity pattern around the wave cloud structure in a simulation study of wave-cloud interaction, Clark et al. (1986) found that gravity waves play an important role in the vertical velocity of air surrounding the cloud. Their simulated clouds have clear air updraughts occurring both in front and overhead on the upshear side and clear downdraughts both in the rear and overhead on the downshear side. They found the persistence of the cloud root updraught in all cases in their simulations, i.e., the persistence of updraught below cloud base. The cloud roots are rather transient in structure and amplitudes in spite of the fact that the boundary layer eddies are quite persistent. They found that the waves and the eddies below cloud bases are more or less coupled to each other in the vertical but do propagate through the cloud field.

Heymsfield and Miloshevich (1995) studied the influence of relative humidity and temperature on cirrus formation and evolution using aircraft measurements. They showed that cloud occurred between the maximum updraught and maximum downdraught. The relative humidity attained its maximum in the middle of the cloud where the temperature was lowest.

Mountain waves and mountain wave clouds have been observed over the British Isles using very high frequency radar (Worthington, 1999), gliders (Stromberg et al., 1989), aircraft measurements (Brown, 1983), radiosondes (Shutts and Broad, 1993), and satellite (Vosper and Parker, 2002). The observational studies have revealed the statistics of mountain wave clouds and the vertical momentum flux which is important for parameterizing gravity wave drag in numerical models. With the advances in aircraft

## Wave cloud

Z. Cui et al.

[Title Page](#)[Abstract](#)[Introduction](#)[Conclusions](#)[References](#)[Tables](#)[Figures](#)[Back](#)[Close](#)[Full Screen / Esc](#)[Printer-friendly Version](#)[Interactive Discussion](#)

**Wave cloud**

Z. Cui et al.

[Title Page](#)[Abstract](#)[Introduction](#)[Conclusions](#)[References](#)[Tables](#)[Figures](#)[I◀](#)[▶I](#)[◀](#)[▶](#)[Back](#)[Close](#)[Full Screen / Esc](#)[Printer-friendly Version](#)[Interactive Discussion](#)

measurements, it is possible to measure the horizontal structure of mountain wave clouds in terms of thermodynamics and microphysics. The Aerosol Properties, Processes And Influences on the Earth's climate (APPRAISE) programme is a Natural Environment Research Council (NERC) funded UK programme aimed at investigating the science of aerosols and their effects on climate. During the APPRAISE-clouds project, aircraft flights were undertaken to measure the cloud dynamical and microphysical properties of a range of cloud types, mainly during the winter-time over the UK (e.g., Crosier et al., 2011; Westbrook and Illingworth, 2011; Crawford et al., 2011). The UK BAe146 Facility for Airborne Atmospheric Measurement (FAAM) aircraft, fitted with a range of state-of-the-art instruments was used to make these observations. On 27 February 2009 (flight designation B432) the aircraft flew through wave clouds over Scotland at several levels ( $T > -5^{\circ}\text{C}$ ) and measured meteorological parameters (e.g., temperature, wind speeds) and cloud properties. There have been no previous reports of wave cloud observations at such high temperatures with detailed in-situ flight measurements. This paper will present the structure of these wave clouds. The results of the study will provide an opportunity for numerical study of the impact of moist processes on mountain waves and wave-cloud interaction with models.

## 2 Instrumentation and flight track

### 2.1 Instruments

The BAe 146 aircraft was equipped with instruments to measure aerosols, microphysics of clouds, dynamics and state parameters of air. The Passive Cavity Aerosol Spectrometer Probe (PCASP), developed by Particle Measuring Systems, Inc., Boulder, Colorado, USA, measures the aerosol size distribution in the nominal range of 0.1 to 3  $\mu\text{m}$ . The Nevzorov LWC-TWC probe is a constant-temperature, hot-wire probe that measures the cloud liquid and total water content. The ice water content can thus be derived. The measurement accuracy of the Nevzorov probe is given as  $\pm 10\text{--}15\%$

**Wave cloud**

Z. Cui et al.

Title Page

Abstract

Introduction

Conclusions

References

Tables

Figures

◀

▶

◀

▶

Back

Close

Full Screen / Esc

Printer-friendly Version

Interactive Discussion



(Korolev et al., 1998). The Johnson-Williams liquid content probe measures liquid water content in clouds using a heated wire resistance bridge at a frequency of 4 Hz. Its operating range is  $0\text{--}3\text{ gm}^{-3}$  and the typical overall uncertainty under normal operation is estimated at  $\pm 10\%$  (Strapp and Schemenauer, 1982). The true air temperature was measured using Rosemount de-iced and non de-iced platinum-resistance immersion thermometers. Overall, for a typical clear air measurement it is estimated to be accurate to  $\pm 0.3^\circ\text{C}$ , but there are additional errors due to sensor wetting or the application of deicing heat (Lawson and Cooper, 1990; Friehe and Khelif, 1992).

The Stratton Park Engineering Company (SPEC) 2D-S-128 shadow imaging probe uses a 128 photodiode linear array to detect 2-D cloud particles passing through the well-defined sample volume. The 2D-S counts and images particles up to 1.3 mm, with a response time about 10 times faster than that of the older 2D-C (cloud) probe. Its greatly improved determination of sample volume and sizing of particles of ( $50\mu\text{m} \leq d \leq 100\mu\text{m}$ ) diameter (Lawson et al., 2006) provides significantly improved measurements of particles of both phase in this important size range. The SPEC Cloud Particle Imaging (CPI) instrument (Lawson et al., 2001), images cloud particles with diameter  $d \approx 5\mu\text{m}$  and larger, although at small sizes ( $d < 50\mu\text{m}$ ) it becomes difficult to use the CPI to distinguish the ice crystal habit of small particles ( $d < 50\mu\text{m}$ ) unambiguously due to having insufficient pixels to determine their shape (Connolly et al., 2007). The Droplet Measurement Technologies (DMT) Cloud Droplet Probe (CDP) is a single-particle instrument that measures the light scattered from a droplet passing through an open path laser beam. The CDP uses a diode laser, with a single mode elliptical Gaussian beam roughly  $2 \times 0.2\text{ mm}$ , to count and size individual water droplets in the diameter range of  $3\text{--}50\mu\text{m}$  (Lance et al., 2010).

## 2.2 Atmospheric conditions and flight pattern

There was a ridge of high pressure over the UK on 27 February 2009 and the flow was westerly over Scotland. Wave clouds were observed in satellite images over Northern Ireland and Scotland on 27 February 2009 (Fig. 1). The vertical profiles of potential

**Wave cloud**

Z. Cui et al.

Title Page

Abstract

Introduction

Conclusions

References

Tables

Figures

◀

▶

◀

▶

Back

Close

Full Screen / Esc

Printer-friendly Version

Interactive Discussion



temperature and wind speed obtained using the 146 are shown in Fig. 2. There was an inversion layer at  $z \approx 1.8$  km. The layer between  $z = 1.6$  km and  $z = 1.8$  km was close to neutral stability, and winds were variable. The wind speed increased with height within the inversion layer and gradually for about another 400 m above the layer. There were maxima at  $z \approx 2250$  m in  $u$  and  $v$  components (of about  $15$  and  $8$   $\text{ms}^{-1}$ , respectively). These conditions favour the formation of cloud bands over the UK (Weston, 1980).

The aircraft flew in the wave clouds over Scotland at several levels. The first run was towards the east at  $z \approx 1.65$  km above sea level. Subsequent runs were carried out after a turn and a short profile ascent (see Fig. 3). The aircraft penetrated the wave clouds during runs 1–4. In runs 5 and 6, the aircraft encountered small lenticular capping clouds formed above the crest of the wave clouds below. Run 7, at  $z \approx 2.6$  km, was in clear air above the clouds. The temperature range in runs 1–6 was between  $4.4$  and  $-4.4$   $^{\circ}\text{C}$ .

### 3 Structure of wave clouds

The first run was at  $z \approx 1.65$  km a.s.l. towards the east. Three clouds were penetrated and these are labelled C1, C2 and C3 in Fig. 4. After C3, the aircraft gently climbed 200 ft because of the rising terrain and continued penetrating clouds C4, C5, C6 and C7. The liquid water contents from three different instruments are shown in Fig. 4a. The maximum values encountered in the clouds were between  $0.3$  and  $0.6$   $\text{gkg}^{-1}$  for the Johnson-Williams probe. The maximum concentrations of cloud particles larger than  $10$   $\mu\text{m}$  measured with CDP were around  $100$   $\text{cm}^{-3}$  (Fig. 4b). The vertical velocity,  $w$ , displays a distinct pattern with respect to the location of clouds. The horizontal wind was from the south-west at this level. The maximum value of  $w$  was on the upshear sides of the clouds and the minima on the downshear sides. The maxima were often measured outside of the clouds. It is clearly seen that the variations of both the vertical velocity and temperature ( $T$ ) are wave-like (Fig. 4c) and that  $T$  and  $w$  are not in phase. The peaks in  $w$  are generally between the peaks and troughs of  $T$ . This structure is

**Wave cloud**

Z. Cui et al.

[Title Page](#)[Abstract](#)[Introduction](#)[Conclusions](#)[References](#)[Tables](#)[Figures](#)[◀](#)[▶](#)[◀](#)[▶](#)[Back](#)[Close](#)[Full Screen / Esc](#)[Printer-friendly Version](#)[Interactive Discussion](#)

the signature of gravity waves, which is consistent with the satellite image (Fig. 1) and existing knowledge of the wave cloud formation mechanism (Holton, 2004). It is noted that measurements of temperature are not accurate within cloud due to wetting effects on the sensor for clouds where  $T > 0^{\circ}\text{C}$  (e.g., Lenschow and Pennell, 1974; Lawson and Cooper, 1990; Eastin et al., 2002). In clouds where  $T < 0^{\circ}\text{C}$ , the deiced probe is subject to a further correction when the deicing heat is applied to the housing. The icing effect on the temperature sensor is minimal even though super-cooled water droplets exist at temperatures greater than  $-5^{\circ}\text{C}$ . However, both the CDP and CPI images suggest there are no ice particles present in these wave clouds. Even in clear air, the gravity wave features are seen between C2 and C3 in Fig. 4 and before C13 in Fig. 8.

The 2D-S data indicate that the diameters of cloud particles were all less than  $180\ \mu\text{m}$ , with the majority of the particles smaller than  $30\ \mu\text{m}$ . The concentrations of particles with  $50 \leq d \leq 150\ \mu\text{m}$  were only a few tens per litre. The cloud particle size distributions obtained from the CDP probe during run 1 are shown in Fig. 5. The highest droplet concentrations were observed in clouds C1–C3 where the drop diameters were generally between  $15\text{--}25\ \mu\text{m}$ . Larger droplet sizes (between  $25\text{--}45\ \mu\text{m}$ ) were observed in clouds C4–C7 where the liquid water contents are higher than in C1–C3. This is illustrated by the calculated mean volume diameters. The size distributions are thus in agreement with the observed LWC and concentrations in Fig. 4, where clouds C1–C3 have lower LWC, compared with clouds C4–C7. To clearly see the size distributions at different locations within the clouds, we have divided up each of the clouds into eight equal parts in the horizontal direction, and then grouped the eight parts into five areas for comparison. These comprise the first and the last areas (first and eighth parts) which are the upshear and downshear regions, respectively. The third area is the core region which occupies the central two (fourth and fifth) parts. The second area covers the two parts (second and third parts) between the upshear and the core regions, and the fourth area (sixth and seventh parts) is between the core and the downshear regions. In each area, the size distributions are averaged to get a mean distribution. The combined size distributions derived from both the CDP and 2D-S data analysed in this

way for run 1 are shown in Fig. 6. The standard deviations are large for clouds C2 and C3. The overlapping of error bars for drop sizes larger than 50  $\mu\text{m}$  indicates that the differences are not significant in clouds C2 and C3. For clouds C4–C7, drop sizes were larger in the inner parts of the clouds than in the flanks. In cloud C5, the largest drops in size were found in the core and further downwind. Another feature of clouds C4–C7 is that more small droplets were found in the two side regions of the clouds. For most clouds, there were more small droplets in the upshear side than in the downshear side.

After a turn and a short profile ascent of 183 m to the next level, the aircraft headed back towards the west for run 2. A series of penetrations (straight and level runs) were then carried out perpendicular to the 2-dimensional crests and troughs of the waves at successively higher altitudes. These were separated by 152 m intervals up to an altitude of about 2.6 km a.s.l. In run 2 (Fig. 7), the vertical velocity with respect to cloud varied in a similar way in clouds C9, C10, and C11 as in clouds C2–C7 in run 1: the maximum of the updraughts were on the upshear side of the clouds and maximum of the downdraughts on the downshear side (see Fig. 7), with a gradual change from one to the other. This feature was exhibited in cloud C13 in run 3 and all clouds in run 4. Figure 7a and b shows that cloud C12 in run 2 was actually comprised of three separate waves with the same characteristic velocity pattern in each part, but without a clear air/cloud-free region between the downdraught and updraught. Interestingly, the reduction in the liquid water content and also in the concentration of droplets did not coincide with the vertical wind as occurred in clouds C9 and C11 in this run, and several clouds in the previous run. It is noted that in cloud C12a there is a dip in the LWC with the dip in vertical velocity. Within the cloud, the vertical velocity shows signs of wave activity (Fig. 7c). It is clear that there were gravity waves within the cloud. The wave activity within clouds was also seen in C14 in run 3 (Fig. 8). It is not clear what the horizontal extent of the cloud was since the eastern boundary of the cloud was beyond the end of the run. It is also noted that waves existed in the clear air to the west of C13 and between C13 and C14 (Fig. 8). The existence of gravity waves was also seen between C2 and C3 in run 1 (Fig. 4) and between C15 and C16 in run 4 (Fig. 9).

## Wave cloud

Z. Cui et al.

[Title Page](#)[Abstract](#)[Introduction](#)[Conclusions](#)[References](#)[Tables](#)[Figures](#)[I◀](#)[▶I](#)[◀](#)[▶](#)[Back](#)[Close](#)[Full Screen / Esc](#)[Printer-friendly Version](#)[Interactive Discussion](#)

## 4 Discussion and conclusion

Observational studies have revealed the importance of gravity waves in cloud dynamics and microphysics (e.g., Heymsfield and Miloshevich, 1993; Gultepe and Starr, 1995; Haag and Kärcher, 2004; Böhme et al., 2004). For a pure gravity wave, the solution (Lin, 2007) can be expressed as

$$w' = w_r \cos(kx + mz - \omega t) - w_i \sin(kx + mz - \omega t) \quad (2)$$

and

$$\theta' = \frac{\theta_0 N^2}{g\omega} [w_r \sin(kx + mz - \omega t) - w_i \cos(kx + mz - \omega t)], \quad (3)$$

where  $w_r$  and  $w_i$  are the real and imaginary parts of  $\tilde{w}$ , respectively. A typical feature for gravity waves is a phase shift of  $90^\circ$  between temperature and vertical velocity, which has been discussed in detail in Lin (2007) and Holton (1992). Figure 10 shows the ideal structure of a wave cloud. There is a phase shift between temperature and vertical velocity. The temperature decreases below the average at the point where the upward motion is strongest, reaches the lowest at the wave crest, and increases to the average where the strongest downward motion is. A vertical displacement  $\Delta z$  in water-vapour-saturated air will give rise to a change in absolute humidity (Aleksandrova et al., 1992)

$$AH = \frac{216}{T} e_s \left( \Lambda \gamma_a - \frac{1}{H} \right) \Delta z, \quad (4)$$

where  $T$  is the average temperature,  $e_s$  is the saturation vapour pressure,  $\Lambda$  is the temperature-dependence parameter of the saturation vapour pressure, and  $\gamma_a$  is the saturated adiabatic lapse rate. Equation (4) suggests an increase in humidity in the wave crest and a decrease in the wave trough.

Title Page

Abstract

Introduction

Conclusions

References

Tables

Figures

◀

▶

◀

▶

Back

Close

Full Screen / Esc

Printer-friendly Version

Interactive Discussion



**Wave cloud**

Z. Cui et al.

[Title Page](#)[Abstract](#)[Introduction](#)[Conclusions](#)[References](#)[Tables](#)[Figures](#)[Back](#)[Close](#)[Full Screen / Esc](#)[Printer-friendly Version](#)[Interactive Discussion](#)

The horizontal distribution of vertical velocity across the wave clouds is different from the definition in the Glossary of Meteorology (Glickman, 2000). We found in our study that the maxima in updraughts on the upshear side and the strong downdraughts on the downshear side. Apparently, most clouds in our case span approximately between the strongest updraught and strongest downdraught. The results of this paper and the previous studies (Durran and Klemp, 1982; Clark et al., 1986; Heymsfield and Miloshevich, 1995) suggest that a wave cloud forms between the maximum updraught and maximum downdraught in the crest of the wave (Fig. 10).

The gaps between clouds are not uniform in our observations. Gravity waves may play their role in the organization and spacing of the wave clouds. The uneven gaps between clouds are very likely caused by the interaction between cloud and gravity wave as suggested by Clark et al. (1986).

In terms of wave-cloud interaction, we did not measure wind below cloud base because of aircraft operating restrictions. Therefore, it is not possible to confirm the persistent cloud root upward eddies (Clark et al., 1986). However, the horizontal dimension of clouds generally decreases with height. The observations at 4 levels in runs 1–4 demonstrate the same features in vertical velocity. This indicates that updraughts occur both in front and overhead on the upshear side and downdraughts both in the rear and overhead on the downshear side of the wave clouds.

There are some questions that need further study in the future. For example, what was the relative contribution to the gravity wave generation from topography, from convection, and from other sources? In runs 2 and 3, waves apparently operated in clouds. It is not known how waves travelled in cloud without significant damping. The interaction between cloud and gravity waves is complex. Clark et al. (1986) noted that “*the persistence of the cloud root updraught is quite apparent in spite of the dramatically changing overhead wave field characteristics*”. In order to better understand the processes, we suggest that measurements (airborne, ground-based or radar) below cloud bases should be carried out in any future wave cloud study.

**Wave cloud**

Z. Cui et al.

[Title Page](#)[Abstract](#)[Introduction](#)[Conclusions](#)[References](#)[Tables](#)[Figures](#)[Back](#)[Close](#)[Full Screen / Esc](#)[Printer-friendly Version](#)[Interactive Discussion](#)

In conclusion, we have analyzed aircraft measurements of wave clouds. We have found that the variations of vertical velocity across wave clouds vary in a distinctive way. The updraughts have maxima on the upshear sides of the clouds and strong down-draughts on the downshear sides. We have also presented the microphysical properties of the clouds. The specific water contents are  $0.3\text{--}0.6\text{ g k}^{-1}$ . The concentrations of cloud particles (all drops) are about a couple of hundreds per cubic centimeters. Cloud particles are generally between  $15\text{--}45\text{ }\mu\text{m}$  in size with only a small proportion reaching drizzle sizes. Previous studies of wave clouds in mixed-phase or ice-phase have made progress in understanding the distribution of ice particles and their relationship with ice nuclei. However, it is well known that the parameterization of ice particle formation is difficult because of various freezing modes. Cloud development is highly dependent on the freezing schemes (e.g., Cui et al., 2011). Moreover, the discrepancy is large between ice nuclei concentration and ice particle concentration, particularly at temperatures greater than  $-10\text{ }^{\circ}\text{C}$  (Pruppacher and Klett, 1997). The results of ice-free wave clouds presented in this paper provide a case with less complexity and less uncertainty for future numerical simulation of wave clouds and of the interaction between wave and cloud.

*Acknowledgements.* The work was funded by the Natural Environment Research Council AP-PRAISE programme, grant number NE/E01125X/1. We would like to thank the DFL pilots and operators of the FAAM BAe146 aircraft and the FAAM staff for assistance in undertaking these measurements with the data and for making the project possible. We also thank NCAS and FGAM for their measurements and operators. We are grateful to the British Atmospheric Data Centre for providing access to the APPRAISE-clouds dataset.

## References

- Aleksandrova, T. V., Plechkov, V. M., and Stankevich, K. S.: Detection of internal gravity waves in cloud layers according to radio-brightness contrasts of the atmosphere, *Radiophys. Quantum El.*, 35, 155–158, doi:10.1007/BF01038019, 1992.
- 5 Baker, B. A. and Lawson, R. P.: In situ observations of the microphysical properties of wave, cirrus, and anvil clouds. Part I: Wave clouds, *J. Atmos. Sci.*, 63, 3160–3185, 2006.
- Baumgardner, D. and Gandrud, B. E.: A comparison of the microphysical and optical properties of particles in an aircraft contrail and mountain wave cloud, *Geophys. Res. Lett.*, 25, 1129–1132, 1998.
- 10 Böhme, T., Hauf, T., and Lehmann, V.: Investigation of short-period gravity waves with the Lindenberg 482 MHz tropospheric wind profiler, *Q. J. Roy. Meteor. Soc.*, 130, 2933–2952, 2004.
- Brown, P. R. A.: Aircraft measurements of mountain waves and their associated momentum flux over the British Isles, *Q. J. Roy. Meteor. Soc.*, 109, 849–865, 1983.
- Clark, T. L. and Hauf, T.: Upshear cumulus development: a result of boundary layer/free atmosphere interactions, in: *Conf. Radar. Meteorol. Conf. Cloud Phys.*, 23rd, Snowmass, Colo., J18–J21, American Meteorological Society, Boston, Massachusetts, Preprints, 1986.
- 15 Clark, T. L., Hauf, T., and Kuettner, J. P.: Convectively forced internal gravity waves: results from two-dimensional experiments, *Q. J. Roy. Meteor. Soc.*, 112, 899–926, 1986.
- Connolly, P. J., Flynn, M. J., Ulanowski, Z., Choullarton, T. W., Gallagher, M. W., and Bower, K. N.: Calibration of the cloud particle imager probes using calibration beads and ice crystal analogs: the depth of field, *J. Atmos. Ocean. Tech.*, 24, 1860–1879, 2007.
- 20 Cooper, W. A. and Saunders, C. P. R.: Winter storms over the San Juan Mountains. Part II: Microphysical processes, *J. Appl. Meteorol.*, 19, 927–941, 1980.
- Cooper, W. A. and Vali, G.: The origin of ice in mountain cap clouds, *J. Atmos. Sci.*, 38, 1244–1259, 1981.
- 25 Cotton, W. R., Bryan, G., and van den Heever, S.: *Storm and Cloud Dynamics*, Academic Press, New York, 820 pp., 2010.
- Crawford, I., Bower, K. N., Choullarton, T. W., Dearden, C., Crosier, J., Westbrook, C., Capes, G., Coe, H., Connolly, P., Dorsey, J. R., Gallagher, M. W., Williams, P., Trembath, J., Cui, Z., and Blyth, A.: Ice formation and development in aged, wintertime cumulus over the UK : observations and modelling, *Atmos. Chem. Phys. Discuss.*, 11, 30797–30851, doi:10.5194/acpd-11-30797-2011, 2011.
- 30

### Wave cloud

Z. Cui et al.

Title Page

Abstract

Introduction

Conclusions

References

Tables

Figures

◀

▶

◀

▶

Back

Close

Full Screen / Esc

Printer-friendly Version

Interactive Discussion



**Wave cloud**

Z. Cui et al.

[Title Page](#)[Abstract](#)[Introduction](#)[Conclusions](#)[References](#)[Tables](#)[Figures](#)[I◀](#)[▶I](#)[◀](#)[▶](#)[Back](#)[Close](#)[Full Screen / Esc](#)[Printer-friendly Version](#)[Interactive Discussion](#)

- Crosier, J., Bower, K. N., Choullarton, T. W., Westbrook, C. D., Connolly, P. J., Cui, Z. Q., Crawford, I. P., Capes, G. L., Coe, H., Dorsey, J. R., Williams, P. I., Illingworth, A. J., Gallagher, M. W., and Blyth, A. M.: Observations of ice multiplication in a weakly convective cell embedded in supercooled mid-level stratus, *Atmos. Chem. Phys.*, 11, 257–273, doi:10.5194/acp-11-257-2011, 2011.
- 5 Cui, Z., Davies, S., Carslaw, K. S., and Blyth, A. M.: The response of precipitation to aerosol through riming and melting in deep convective clouds, *Atmos. Chem. Phys.*, 11, 3495–3510, doi:10.5194/acp-11-3495-2011, 2011.
- Durrán, D. R. and Klemp, J. B.: The effects of moisture on trapped mountain lee waves, *J. Atmos. Sci.*, 39, 2490–2506, 1982.
- 10 Eastin, M. D., Black, P. G., and Gray, W. M.: Flight-level thermodynamic instrument wetting errors in hurricanes. Part I: Observations, *Mon. Weather Rev.*, 130, 825–841, 2002.
- Field, P. R., Cotton, R. J., Noone, K., Glantz, P., Kaye, P. H., Hirst, E., Greenaway, R. S., Jost, C., Gabriel, R., Reiner, T., Andreae, M., Saunders, C. P. R., Archer, A., Choullarton, T., Smith, M., Brooks, B., Hoell, C., Bandy, B., Johnson, D., and Heymsfield, A.: Ice nucleation in orographic wave clouds: measurements made during INTACC, *Q. J. Roy. Meteor. Soc.*, 127, 1493–1512, 2001.
- 15 Friehe, C. A. and Khelif, D.: Fast-response aircraft temperature sensors, *J. Atmos. Ocean. Tech.*, 9, 784–795, 1992.
- 20 Glickman, T. S.: *Glossary of Meteorology*, 2nd edn., American Meteorological Society, Boston, MA, 2000.
- Gultepe, I. and Starr, D. O.: Dynamical structure and turbulence in cirrus clouds: aircraft observations during FIRE, *J. Atmos. Sci.*, 52, 4159–4182, 1995.
- Heymsfield, A. J. and Miloshevich, L. M.: Relative humidity and temperature influences on cirrus formation and evolution: observations from wave clouds and FIRE-II, *J. Atmos. Sci.*, 52, 4302–4323, 1995.
- 25 Haag, W. and Kärcher, B.: The impact of aerosols and gravity waves on cirrus clouds at midlatitudes, *J. Geophys. Res.*, 109, D12202, doi:10.1029/2004JD004579, 2004.
- Holton, J.: *An introduction to dynamic meteorology*, Academic Press, London, 4th Edn., 2004.
- 30 Jensen, E. J., Toon, O. B., Tabazadeh, A., Sachse, G. W., Anderson, B. E., Chan, K. R., Twohy, C. W., Gandrud, B., Aulenbach, S. M., Heymsfield, A., Hallett, J., and Gary, B.: Ice nucleation processes in upper tropospheric wave-clouds observed during SUCCESS, *Geophys. Res. Lett.*, 25, 1363–1366, 1998.

**Wave cloud**

Z. Cui et al.

[Title Page](#)[Abstract](#)[Introduction](#)[Conclusions](#)[References](#)[Tables](#)[Figures](#)[◀](#)[▶](#)[◀](#)[▶](#)[Back](#)[Close](#)[Full Screen / Esc](#)[Printer-friendly Version](#)[Interactive Discussion](#)

- Korolev, A. V., Nevzorov, A. N., Strapp, J. W., and Isaac, G. A.: The Nevzorov airborne hot-wire LWC-TWC probe: principle of operation and performance characteristics, *J. Atmos. Ocean. Tech.*, 15, 1495–1510, 1998.
- 5 Kuettner, J. P., Hildebrand, P. A., and Clark, T. L.: Convection waves: observations of gravity wave systems over convectively active boundary layers, *Q. J. Roy. Meteor. Soc.*, 113, 445–467, 1987.
- Lance, S., Brock, C. A., Rogers, D., and Gordon, J. A.: Water droplet calibration of the Cloud Droplet Probe (CDP) and in-flight performance in liquid, ice and mixed-phase clouds during ARCPAC, *Atmos. Meas. Tech.*, 3, 1683–1706, doi:10.5194/amt-3-1683-2010, 2010.
- 10 Lawson, R. P. and Cooper, W. A.: Performance of some airborne thermometers in clouds, *J. Atmos. Ocean. Tech.* 7, 480–494, 1990.
- Lawson, P. R., Baker, B. A., Schmitt, C. G., and Jensen, T. L.: An overview of microphysical properties of Arctic clouds observed in May and July 1998 during FIRE ACE, *J. Geophys. Res.-Atmos.*, 106 (D14), 14989–15014, 2001.
- 15 Lawson, R. P., O'Connor, D., Zmarzly, P., Weaver, K., Baker, B. A., Mo, Q., and Jonsson, H.: The 2-D-S (stereo) probe: design and preliminary tests of a new airborne, high-speed, high-resolution imaging probe, *J. Atmos. Ocean. Tech.*, 23, 1462–1477, 2006.
- Lenschow, D. H. and Pennell, W. T.: On the measurement of in-cloud and wet-bulb temperatures from an aircraft, *Mon. Weather Rev.*, 102, 447–454, 1974.
- 20 Lin, Y. L.: *Mesoscale dynamics*, Cambridge University Press, Cambridge, 630 pp., 2007.
- Ludlam, F. H.: *Clouds and Storms*, Pennsylvania State University Press, University Park, PA, 1980.
- Politovich, M. K. and Vali, G.: Observations of liquid water in orographic clouds over Elk Mountain, *J. Atmos. Sci.*, 40, 1300–1312, 1983.
- 25 Pruppacher, H. R. and Klett, J. D.: *Microphysics of Clouds and Precipitation*, 2nd Edn., Kluwer Academic Publishers, Boston, 954 pp., 1997.
- Scorer, R. S.: Theory of waves in the lee of mountains, *Q. J. Roy. Meteor. Soc.*, 75, 41–56, 1949.
- Shutts, G. and Broad, A.: A case study of lee waves over the Lake District in Northern England, *Q. J. Roy. Meteor. Soc.*, 119, 377–408, 1993.
- 30 Strapp, J. W. and Schemenauer, R. S.: Calibrations of Johnson–Williams liquid water content meters in a high-speed icing tunnel, *J. Appl. Meteorol.*, 21, 98–108, 1982.

**Wave cloud**

Z. Cui et al.

[Title Page](#)[Abstract](#)[Introduction](#)[Conclusions](#)[References](#)[Tables](#)[Figures](#)[I◀](#)[▶I](#)[◀](#)[▶](#)[Back](#)[Close](#)[Full Screen / Esc](#)[Printer-friendly Version](#)[Interactive Discussion](#)

Stromberg, I. M., Mill, C. S., Choularton, T. W., and Gallagher, M. W.: A case study of stably stratified airflow over the Pennines using an instrumented glider, *Bound.-Lay. Meteorol.*, 46, 153–168, 1989.

Twohy, C. H., Schanot, A. J., and Cooper, W. A.: Measurement of condensed water content in liquid and ice clouds using an airborne counterflow virtual impactor, *J. Atmos. Ocean. Tech.*, 14, 197–202, 1997.

Vosper, S. B. and Parker, D. J.: Some perspectives on wave clouds, *Weather*, 57, 3–8, 2002.

Weston, K. J.: An observational study of convective cloud streets, *Tellus*, 32, 433–438, 1980.

Westbrook, C. D. and Illingworth, A. J.: Evidence that ice forms primarily in super-cooled liquid clouds at temperatures  $> -27^{\circ}\text{C}$ , *Geophys. Res. Lett.*, 38, L14808, doi:10.1029/2011GL048021, 2011.

Wood, N.: Wind flow over complex terrain: a historical perspective and the prospect for large-eddy modelling, *Bound.-Lay. Meteorol.*, 96, 11–32, 2000.

Worthington, R.: Alignment of mountain wave patterns above Wales: a VHF radar study during 1990–1998, *J. Geophys. Res.*, 104, 9199–9212, 1999.

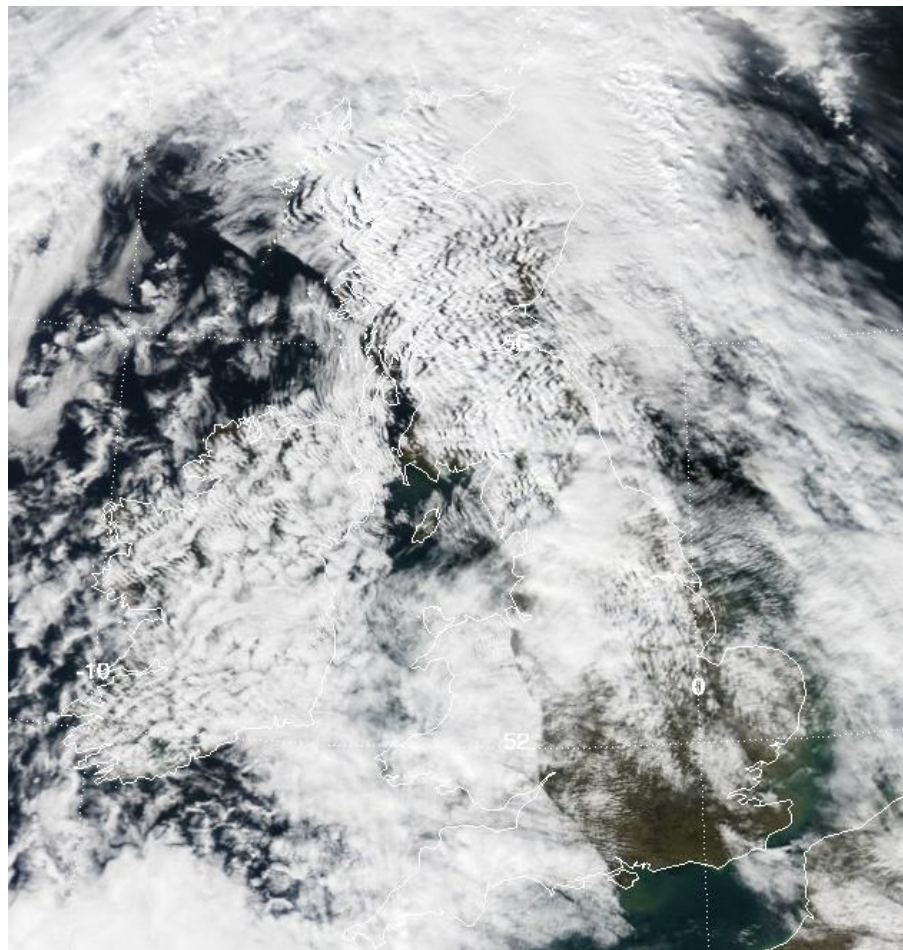


**Fig. 1.** Visible satellite image MODIS for the UK at 13:05 UTC on 27 February 2009.

**Wave cloud**

Z. Cui et al.

Title Page

Abstract

Introduction

Conclusions

References

Tables

Figures

◀

▶

◀

▶

Back

Close

Full Screen / Esc

Printer-friendly Version

Interactive Discussion



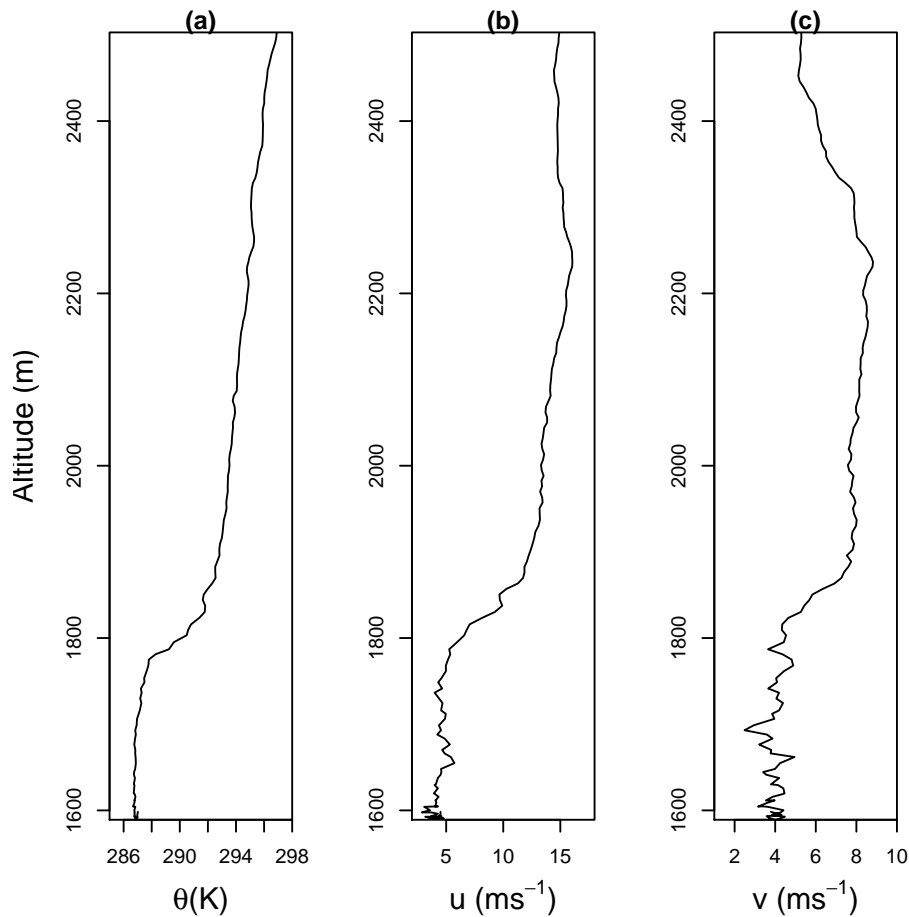


**Fig. 2.** Profiles of potential temperature **(a)**, horizontal wind speeds **(b and c)** sampled by the BAe 146.

**Wave cloud**

Z. Cui et al.

Title Page

|             |              |
|-------------|--------------|
| Abstract    | Introduction |
| Conclusions | References   |
| Tables      | Figures      |

|      |       |
|------|-------|
| ◀    | ▶     |
| ◀    | ▶     |
| Back | Close |

Full Screen / Esc

Printer-friendly Version

Interactive Discussion



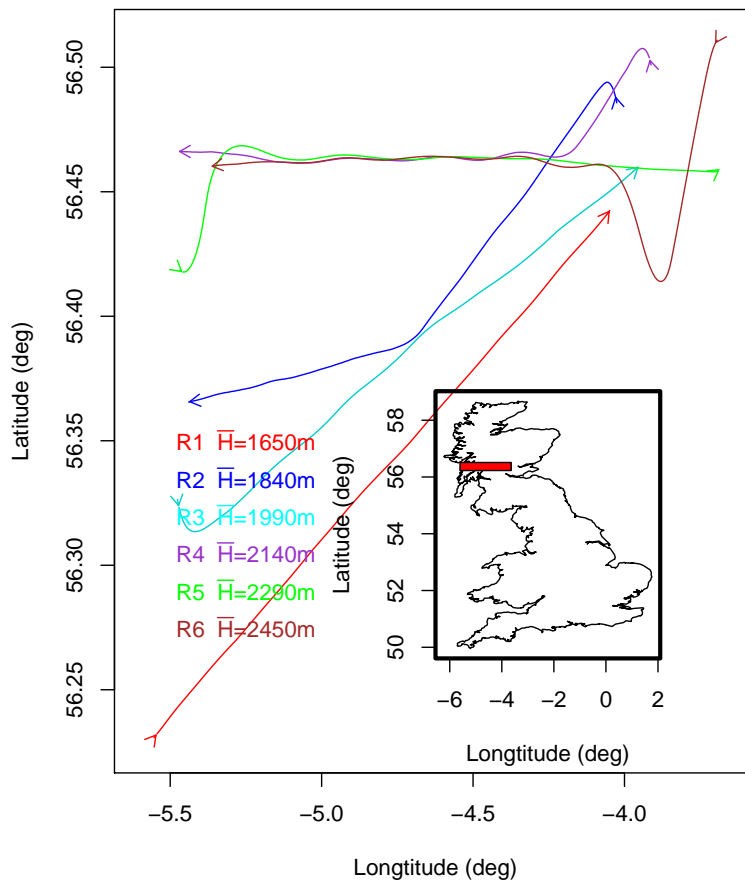


**Fig. 3.** Flight track of runs 1–6 and the mean altitude of each run. The red box in the inset shows the location of the figure. Please note the figure is not in proportion in terms of distance in latitudinal and longitudinal directions.

Title Page

Abstract

Introduction

Conclusions

References

Tables

Figures

◀

▶

◀

▶

Back

Close

Full Screen / Esc

Printer-friendly Version

Interactive Discussion



## Wave cloud

Z. Cui et al.

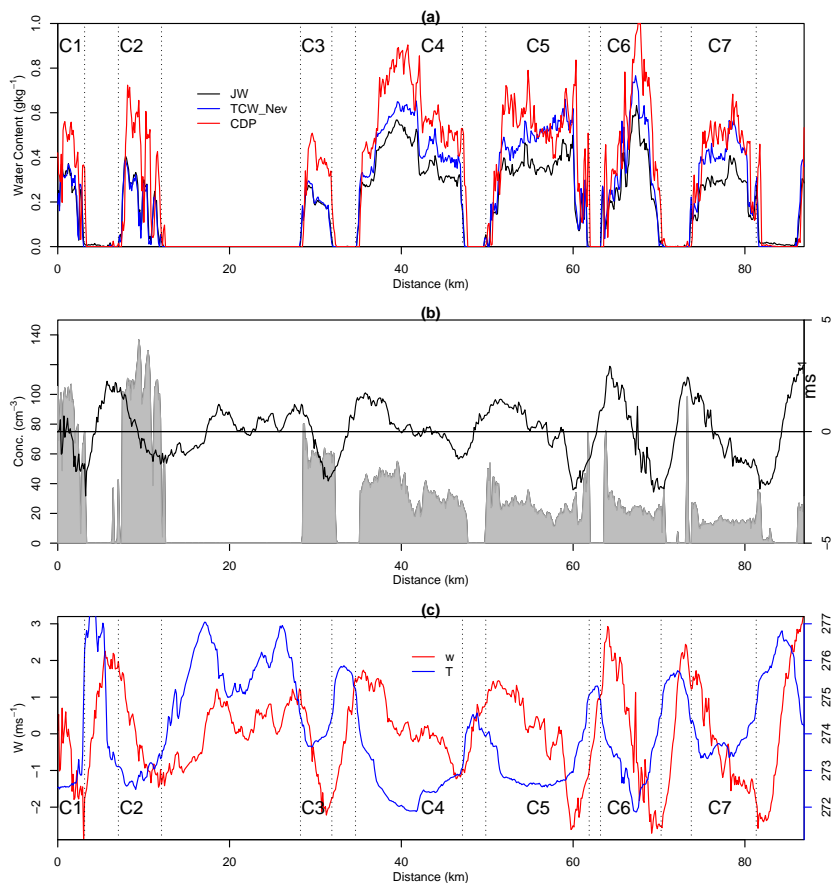


**Fig. 4.** (a) The LWC measured by the Johnson-Williams probe, the Nevzorov total cloud water, and as derived from the CDP, (b), concentration with CDP in grey shade and vertical velocity in black curve (b), and vertical velocity in red and temperature in blue (c) in run 1.

## Wave cloud

Z. Cui et al.

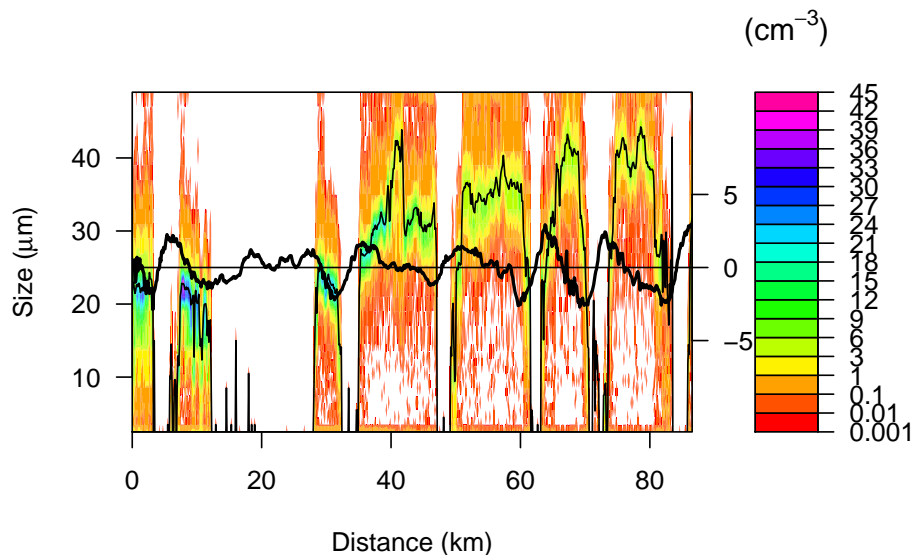


**Fig. 5.** Size distribution function (filled contour) obtained from CDP data for run 1, vertical velocity (thick black curve) and the mean volume diameter (thin black curve).

[Title Page](#)[Abstract](#)[Introduction](#)[Conclusions](#)[References](#)[Tables](#)[Figures](#)[◀](#)[▶](#)[◀](#)[▶](#)[Back](#)[Close](#)[Full Screen / Esc](#)[Printer-friendly Version](#)[Interactive Discussion](#)

## Wave cloud

Z. Cui et al.

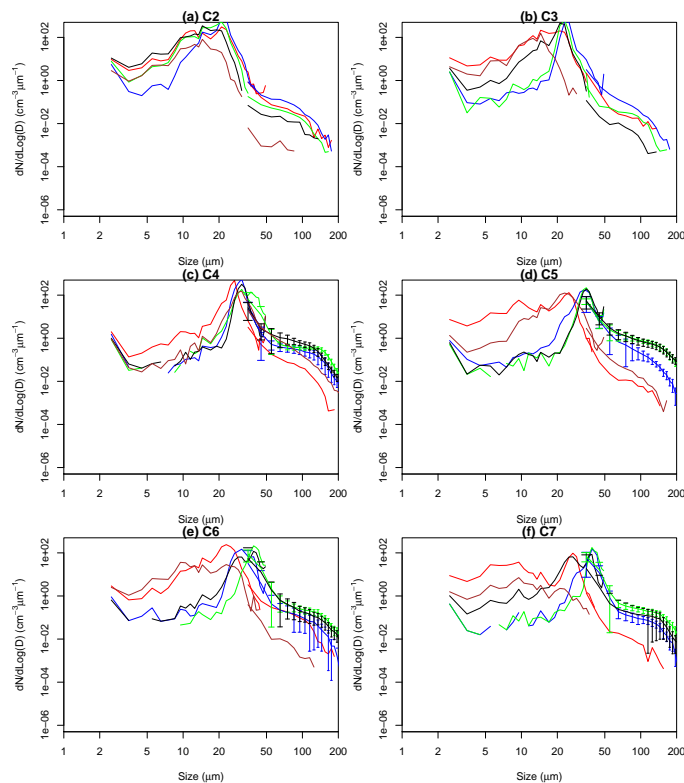


**Fig. 6.** Integrated size distribution of cloud particles from CDP and 2D-S for clouds 2–7. The traverse of a cloud is divided equally to 8 parts in the horizontal direction. The averaged distributions in five areas are shown for each cloud. These 5 areas are: the first part (the upshear side, in red), the second and the third parts (in blue), the 4th and the 5th parts (the cloud core, in green), the 6th and 7th parts (in black), and the 8th part (the downshear side, in brown). The ranges of standard deviation are added for clouds C4–C7 for particles larger than 50  $\mu\text{m}$ .

[Title Page](#)
[Abstract](#)
[Introduction](#)
[Conclusions](#)
[References](#)
[Tables](#)
[Figures](#)
[◀](#)
[▶](#)
[◀](#)
[▶](#)
[Back](#)
[Close](#)
[Full Screen / Esc](#)
[Printer-friendly Version](#)
[Interactive Discussion](#)


Wave cloud

Z. Cui et al.

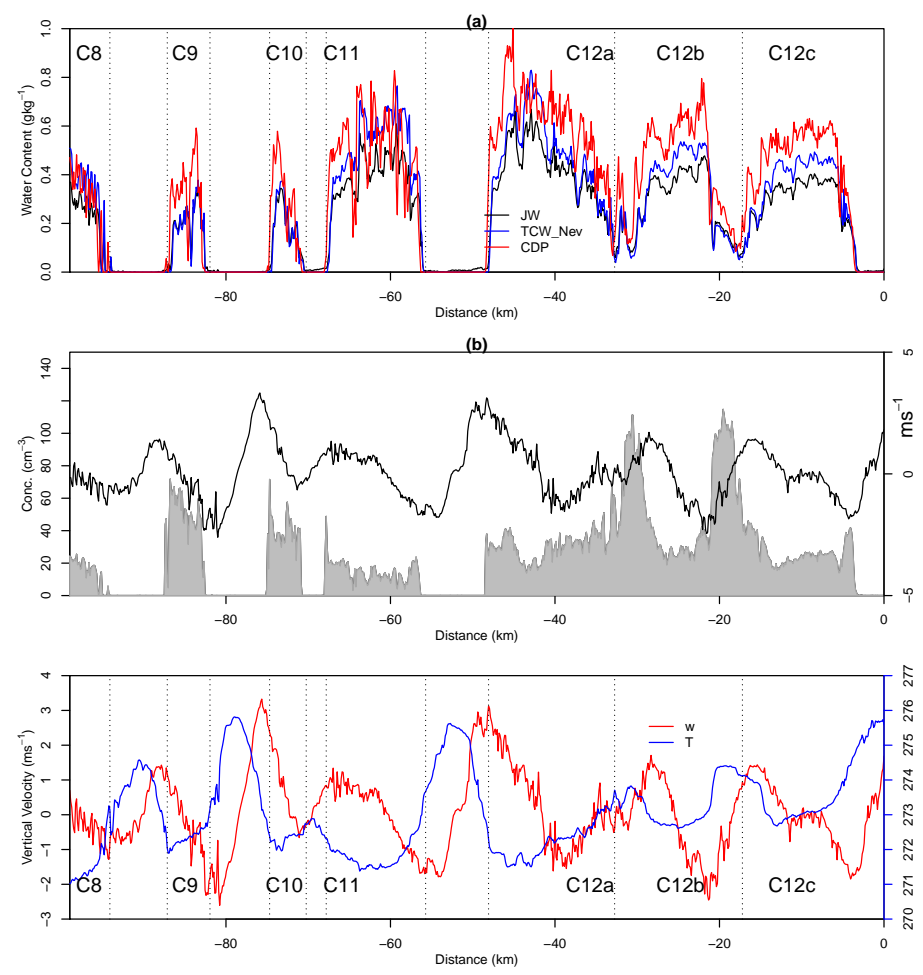


Fig. 7. As in Fig. 4 but for run 2.

Title Page

|             |              |
|-------------|--------------|
| Abstract    | Introduction |
| Conclusions | References   |
| Tables      | Figures      |

◀
▶

◀
▶

|      |       |
|------|-------|
| Back | Close |
|------|-------|

Full Screen / Esc

Printer-friendly Version

Interactive Discussion



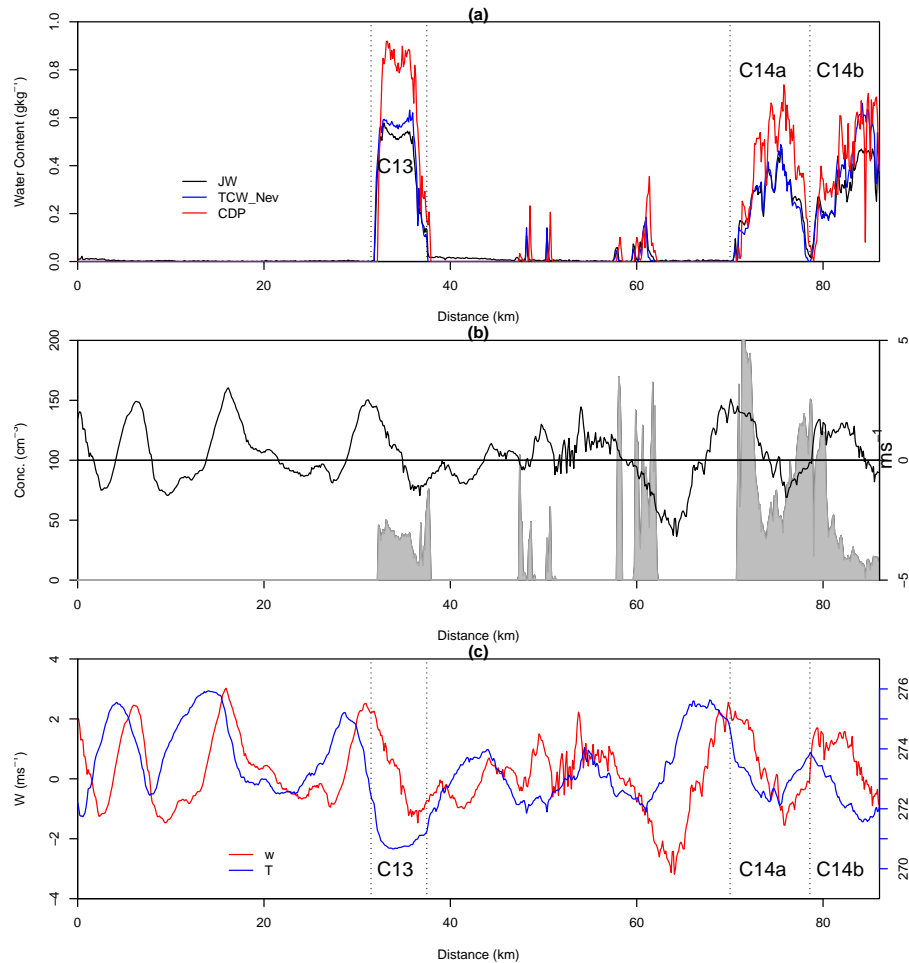


Fig. 8. As in Fig. 4 but for run 3.

Title Page

Abstract

Introduction

Conclusions

References

Tables

Figures

◀

▶

◀

▶

Back

Close

Full Screen / Esc

Printer-friendly Version

Interactive Discussion



**Wave cloud**

Z. Cui et al.

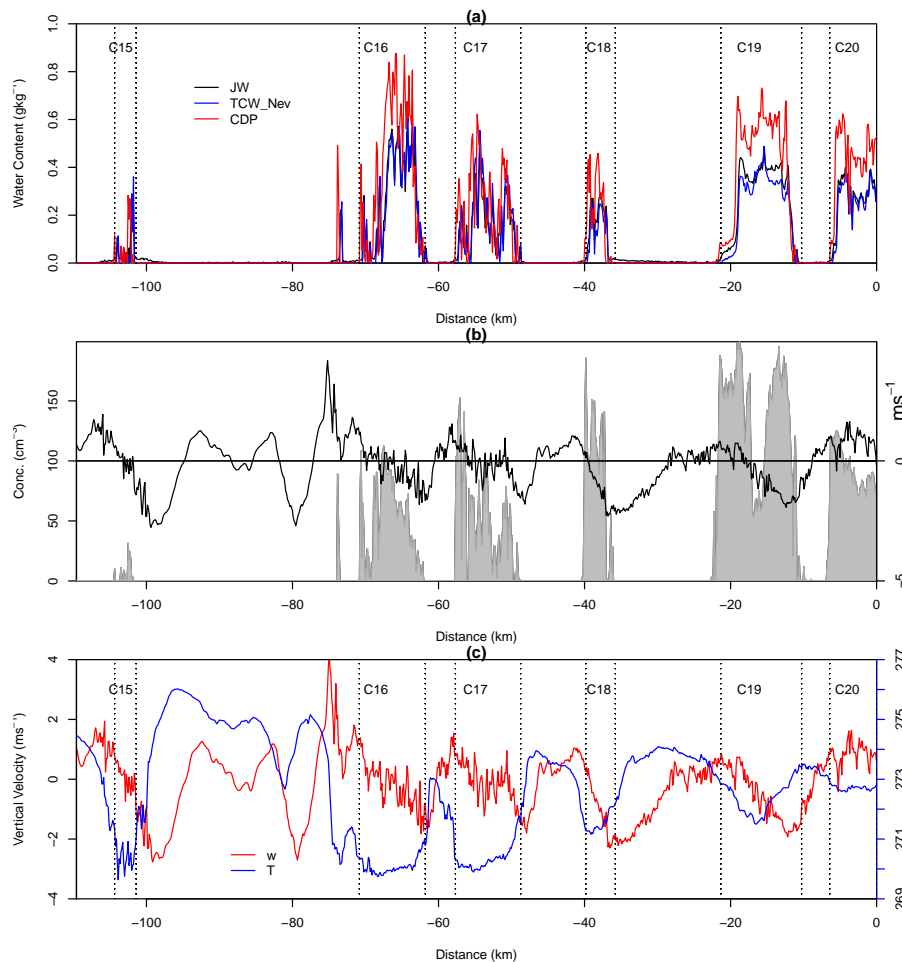


**Fig. 9.** As in Fig. 5 but for run 4.

Title Page

Abstract

Introduction

Conclusions

References

Tables

Figures



Back

Close

Full Screen / Esc

Printer-friendly Version

Interactive Discussion



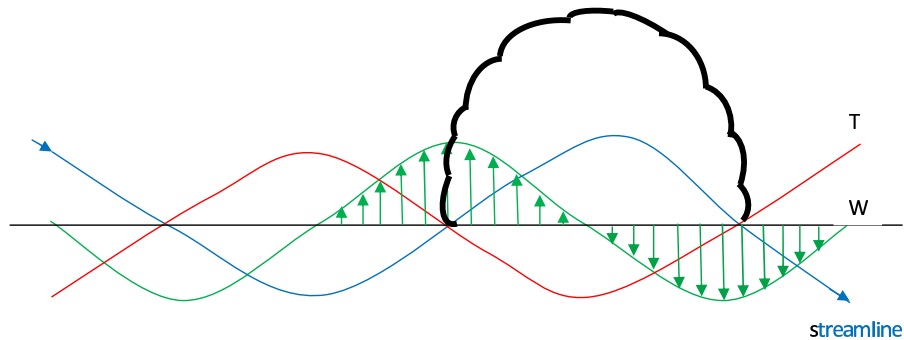


**Fig. 10.** Ideal structure of a wave cloud. The cloud occurs between the maximum and minimum of vertical velocity, where the temperatures are below the undisturbed mean value.

**Wave cloud**

Z. Cui et al.

Title Page

Abstract

Introduction

Conclusions

References

Tables

Figures

◀

▶

◀

▶

Back

Close

Full Screen / Esc

Printer-friendly Version

Interactive Discussion

